

SUPPLEMENTARY INFORMATION

Introducing asymmetric functionality to MOFs via generation of metallic Janus MOF particles

Abraham Ayala, Carlos Carbonell, Inhar Imaz and Daniel Maspoch

Experimental details

Materials

All reagents and solvents used were purchased from Sigma Aldrich and used without further purification.

Synthesis of ZIF-8 Particles (size = $1.3 \pm 0.2 \mu\text{m}$)

A solution of 2-methylimidazole (Hmim; 810.6 mg; 9.9 mM) and 1-methylimidazole (1-Hmim; 810.6 mg (9.9 mM) in 50 mL of MeOH was poured into a solution of $\text{Zn}(\text{NO}_3)_2 \cdot 6\text{H}_2\text{O}$ (734.4 mg; 2.5 mM) in 50 mL of MeOH under magnetic stirring. Stirring was stopped just after both solutions had been mixed. The resulting mixture was kept at room temperature for 24 h. A white precipitate was collected by centrifugation (16775 x g), washed with MeOH, and dried under reduced pressure.¹

Synthesis of ZIF-8 Particles (size = $201 \pm 9 \text{ nm}$)

A solution of $\text{Zn}(\text{NO}_3)_2 \cdot 6\text{H}_2\text{O}$ (1116 mg; 15.0 mM) in 250 mL of MeOH was added into a solution of Hmim (308 mg; 15.0 mM) in 250 mL of MeOH. The mixture was heated at 50 °C for 2 h, and then cooled down to room temperature. The resulting white precipitate was collected by centrifugation (16775 x g), washed with MeOH, and dried under reduced pressure.²

Synthesis of ZIF-8 Particles (size = $101 \pm 10 \text{ nm}$)

A solution of $\text{Zn}(\text{NO}_3)_2 \cdot 6\text{H}_2\text{O}$ (1116 mg; 15.0 mM) in 250 mL of MeOH was added into a solution of Hmim (308 mg; 15.0 mM) in 250 mL of MeOH. The mixture was heated at 50 °C for 1 h, and then cooled down to room temperature. The resulting white precipitate was collected by centrifugation (16775 x g), washed with MeOH, and dried under reduced pressure.²

Synthesis of UiO-66 Particles

A mixture of ZrCl_4 (34.9 mg; 15.0 mM), terephthalic acid (24.9 mg; 15.0 mM) and acetic acid (0.69 mL; 1.2 M) in 8 mL of DMF was heated at 120 °C for 12 h. The resulting solid was collected by centrifugation (16775 x g), washed three times with DMF and MeOH, and dried under reduced pressure.³

Synthesis of UiO-66-SH Particles

2,5-dimercapto-1,4-benzenedicarboxylic acid (BDC-SH) was synthesized as previously reported.⁴ Then, a mixture of $ZrCl_4$ (18.5 mg; 19.3 mM), BDC-SH (9.3 mg; 10.0 mM) and acetic acid (1.3 mL; 2.4 M) in 8 mL of DMF was heated at 120 °C for 12 h. The resulting solid was collected by centrifugation (16775 x g), washed three times with DMF and MeOH, and dried under reduced pressure.⁵

Synthesis of Metallic Janus MOF Particles

Once the different MOF particles were synthesized, the metallic Janus MOF particles was fabricated in three steps:

Steps #1 and #2. Deposition of the MOF particles on Au surfaces. This process started with formation of colloidal dispersions of the different MOF particles. These colloids were prepared by sonicating the synthesized MOF particles (60 mg) in DMF (100 mL) for 15 min. Note that, in the case of UiO-66, these particles (122 mg) were first exposed to polyvinylpyrrolidone (PVP, Mw = 40000, 230 mg) in H₂O (15 mL) under stirring overnight, collected by centrifugation (16775 x g), washed four times with H₂O, once with MeOH, and finally, dried under reduced pressure.³ In parallel, polycrystalline Au films were prepared by E-beam evaporation (ATC-Orion-8E UHV) of 5 nm of Ti on SiO_x surfaces (4 cm²) at a rate of 1 Å/s followed by 40 nm of Au at a rate of 3 Å/s, and a base pressure better than 1x10⁻⁶ Torr. Then, a monolayer of 4-mercaptobenzoic acid (MBA) was fabricated on top of these substrates by immersing them in a 0.1 mM ethanol solution overnight followed by copious rinsing with ethanol. Deprotonation of MBA was achieved by immersing the substrates in an aqueous solution of NaOH (0.1 % w/w) for 20 min, washed several times with H₂O and air-dried. Finally, to deposit these MOF particles, a colloidal MOF solution in DMF (0.15 mL) was spread onto the surfaces, which were then heated at 60 °C until the DMF had evaporated. Here, we made a strategic decision to carefully cover the surface with a true monolayer (even though some areas remained uncovered) rather than to fully cover the surface and risk forming MOF aggregates or multilayers, as any MOF particles underneath the resultant top layer would not be covered in the subsequent next stage.

Step #3. E-beam evaporation of metals on the MOF particles. Polycrystalline Au, Co and Pt films were prepared on the MOF particles by E-beam evaporation (ATC-Orion-8E UHV) of these metals at a rate of 1 Å/s (for thicknesses of 5 nm, 10 nm and 20 nm) or 3 Å/s (for thicknesses of 30 nm or 50 nm) and a base pressure greater than 1x10⁻⁶ Torr.

Step #4. Detachment of metallic Janus MOF particles. In a final step, the synthesized Janus M@MOF particles were detached from the surfaces by ultrasonication (37 KHz, Elma S 30 H Elmasonic) of the surfaces in MeOH for 30 s.

Asymmetric Functionalization of Janus Au@ZIF-8 Particles

Janus Au@ZIF-8 particles were first dispersed into a solution of FITC-PEG-SH (Mw = 3400; 0.3 mM) in 0.5 mL of water by ultrasonication (1 min). The resulting mixture was then incubated at 4 °C for 24 h. Finally, the functionalized Janus particles were collected by centrifugation (16775 x g), cleaned twice with methanol, and finally, redispersed in methanol.

Hg²⁺ adsorption studies

To first determine the sorption equilibrium, several aliquots of Janus Co@UiO-66-SH particles (2 mg) were redispersed into a solution of HgCl₂ (10 ppm of Hg²⁺) in water (4 mL) by ultrasonication for 30 s. The resulting suspensions were then stirred using a vortex period for a certain period of time (0.5 h, 1 h, 2 h, 4 h, or 8 h), and the particles were recollected magnetically. After collection of the particles, the Hg²⁺ content in the solutions was determined by ICP analysis (Table S1). From this experiment, we determined that around 99 % of the Hg²⁺ had already been adsorbed within 30 min.

Table S1. Hg²⁺ content in the solutions after the adsorption process.

Time	Concentration of Hg ²⁺ (ppm)
0.5 h	0.086
1 h	0.090
2 h	0.108
4 h	0.129
8 h	0.109

Motorized Janus Pt@ZIF-8 particles

Janus Pt@ZIF-8 particles (ZIF-8 size = ~ 8 μm; Pt thickness = 60 nm) were prepared following the above-mentioned method. Then, few selected particles were picked up one-by-one with a modified Nanolithography System (NLP200, NanoInk, USA) and positioned on a glass slide. 600 μL of a solution containing 25% of H₂O (pH = 11 adjusted with NaOH 5 M), 25 % of sodium cholate C₂₄H₃₉NaO₅·xH₂O (aqueous solution 15%), 25% of EtOH and 25% of H₂O₂ (20 % in water) was delivered over the area where the particles were previously deposited. After adding this solution, the motion of the Janus Pt@ZIF-8 particles was recorded using an Inverted Optical microscope (Olympus IX71, Japan). The speed was measured using 20 frames and ImageJ software.

Characterization

Field-emission scanning electron microscopy (FESEM) images were collected on a scanning electron microscope (FEI Magellan 400L XHR) at acceleration voltage of 2.0 kV, using aluminium as support. The size of crystals was calculated from FESEM images by averaging the diameter of at least 200 particles from images of different areas of the same samples. High angle annular dark field scanning transmission electron microscope (HAADF-STEM) images and EDX composition profiles were

collected on a Transmission Electron Microscopy (TEM; FEI Tecnai G2 F20) at 200 KV. X-ray powder diffraction (XRPD) measurements were performed using an X'Pert PRO MPDP analytical diffractometer. Volumetric N₂ sorption isotherms were collected at 77 K using a Quantachrome Instrument. As reported by Yaghi *et al.* [K. S. Park, Z. Ni, A. P. Côté, J. Y. Choi, R. Huang, F. J. Uribe-Romo, H. K. Chae, M. O'Keeffe, O. M. Yaghi, Proc. Natl. Acad. Sci. U. S. A. 2006, 103, 10186-10191], calculation of the BET area using the last step leads to high BET values but are likely unreliable (negative C constant). Thus, BET areas (S_{BET}) were calculated (using Quantachrome®ASiQwin software) from the first step of the isotherms, leading to significantly lower but reliable BET values. Superconducting Quantum Interference Device (SQUID) measurements were recorded on a Quantum design MPMS XL-7T (SQUID 7T) instrument at 300 K, and confocal fluorescence images were collected using a confocal microscope (Olympus Fluoview 1000). ICP-MS measurements were performed using an ICP_MS Agilent Serie 7500.

References

- (1) Cravillon, J.; Nayuk, R.; Springer, S.; Feldhoff, A.; Huber, K.; Wiebcke, M. *Chem. Mater.* **2011**, *23*, 2130.
- (2) Chen, L.; Peng, Y.; Wang, H.; Gu, Z.; Duan, C. *Chem. Commun.* **2014**, No. 3, 1.
- (3) Lu, G.; Cui, C.; Zhang, W.; Liu, Y.; Huo, F. *Chem. Asian J.* **2013**, *8*, 69.
- (4) Lamar Field.; Philip, R. E. *J. Org. Chem* **1970**, *35* (11), 3647.
- (5) Yee, K.-K.; Reimer, N.; Liu, J.; Cheng, S.-Y.; Yiu, S.-M.; Weber, J.; Stock, N.; Xu, Z. *J. Am. Chem. Soc.* **2013**, *135*, 7795.

Figure S1. Representative FESEM images of the synthesized colloidal MOFs and corresponding plot of the statistical analysis of their crystal size. (a) ZIF-8 (size = $1.3 \pm 0.2 \mu\text{m}$), (b) ZIF-8 (size = $201 \pm 9 \text{ nm}$), (c) ZIF-8 (size = $101 \pm 10 \text{ nm}$), (d) UiO-66 (size = $190 \pm 22 \text{ nm}$), and (e) UiO-66-SH (size = $208 \pm 54 \text{ nm}$). Scale bars: $10 \mu\text{m}$ (a-e, left image), $3 \mu\text{m}$ (a, right image) and 500 nm (b-e, right image).

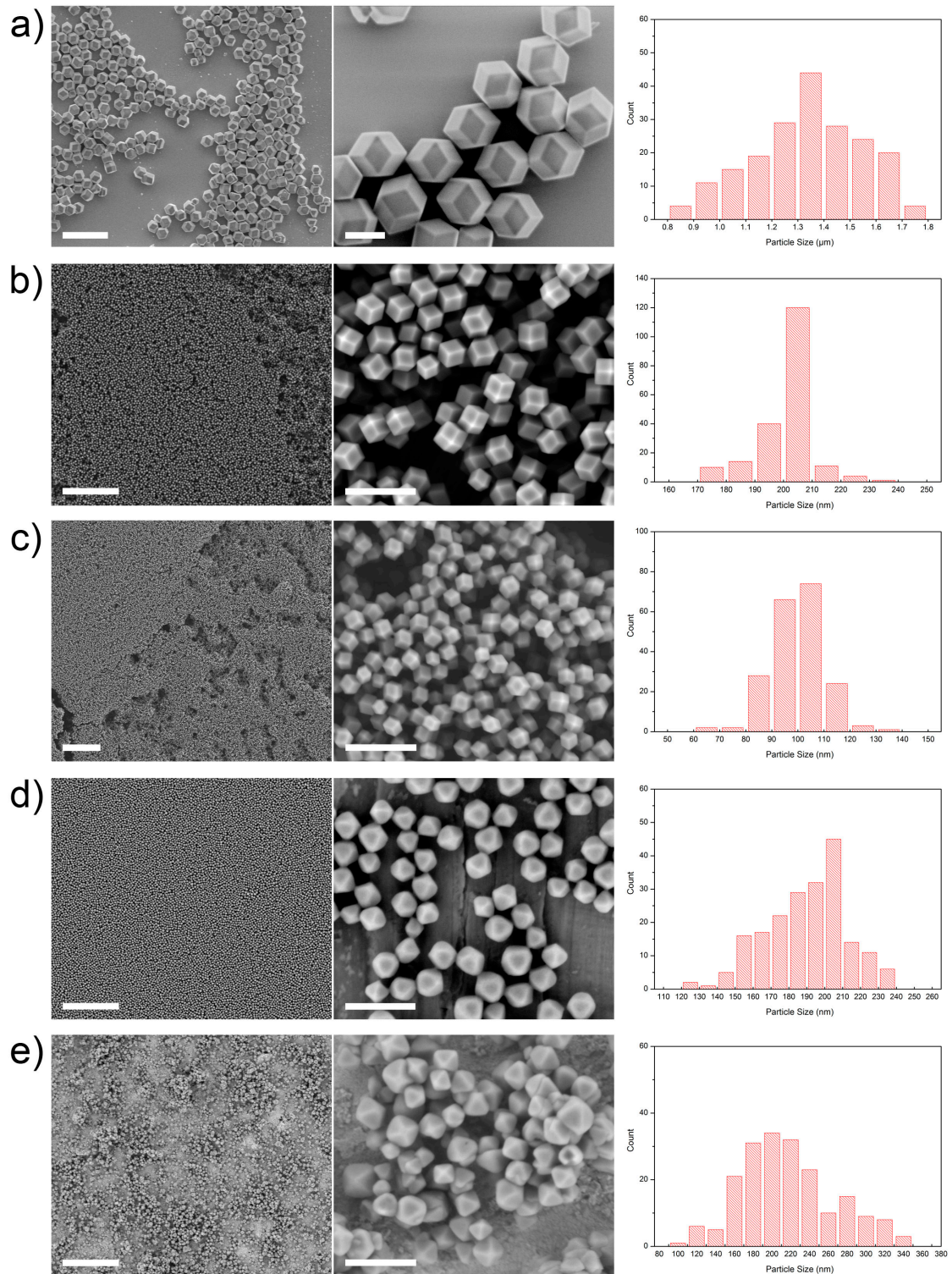
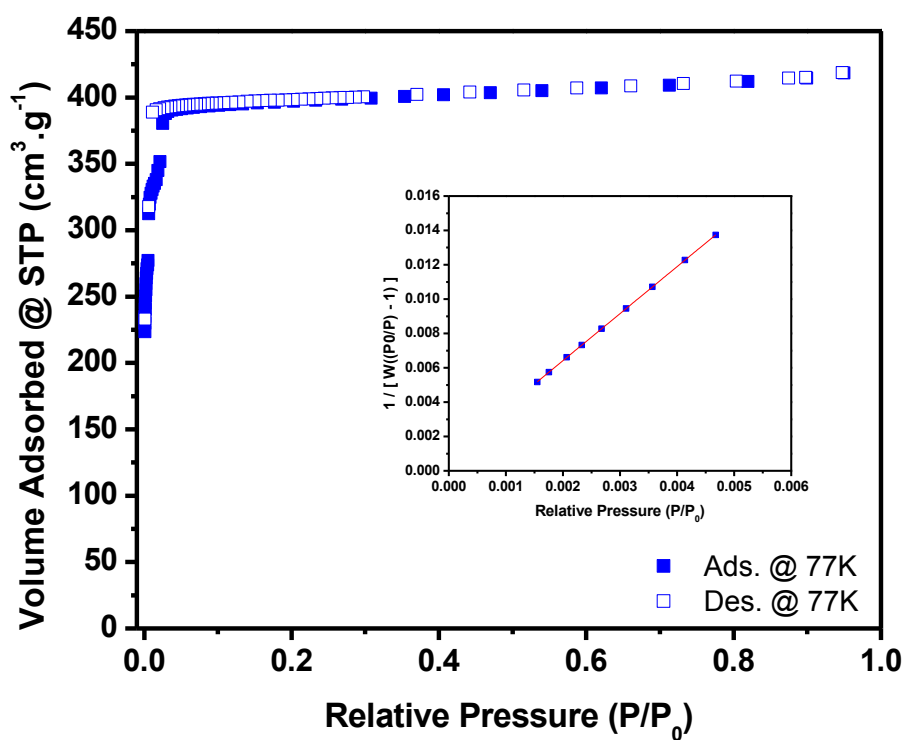


Figure S2. N₂ adsorption isotherm at 77 K. Inset: BET linear fit for ZIF-8 (size = 101 ± 10 nm) crystals.



BET surface area: 1271.824 m²/g STP

Slope: 2.737 g/cm³ STP

Y intercept: 0.0009417 g/cm³ STP

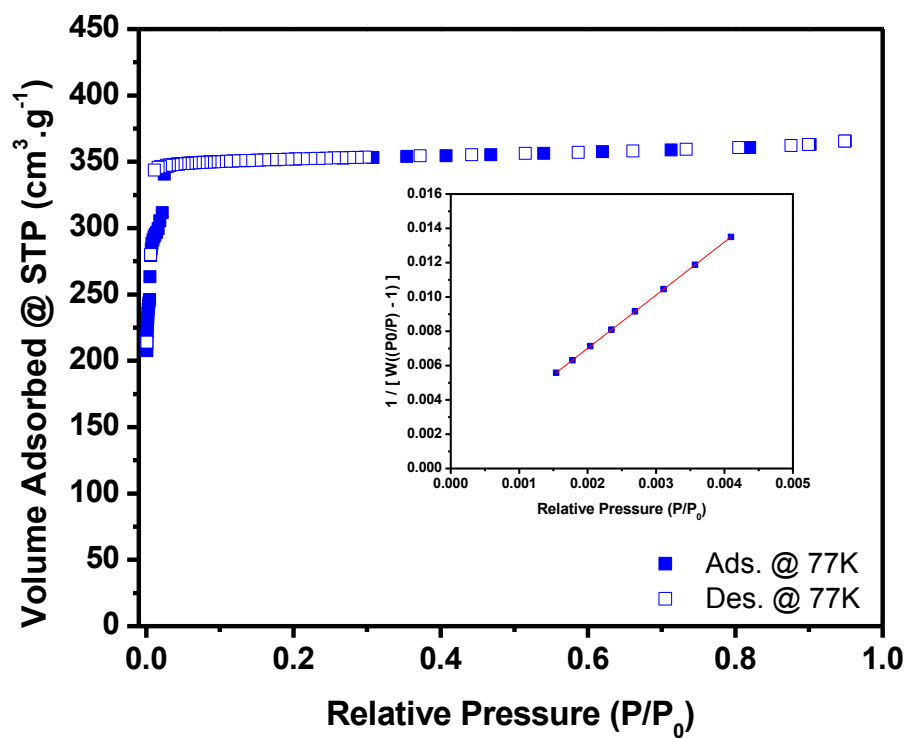
C: 2907.737

Qm: 418.5 cm³/g STP

Correlation Coefficient: 0.999995

Molecular cross sectional area: 0.1620 nm²

Figure S3. N₂ adsorption isotherm at 77 K. Inset: BET linear fit for ZIF-8 (size = 201 ± 9 nm) crystals.



BET surface area: 1122.986 m²/g STP

Slope: 3.100 g/cm³ STP

Y intercept: 0.0008054 g/cm³ STP

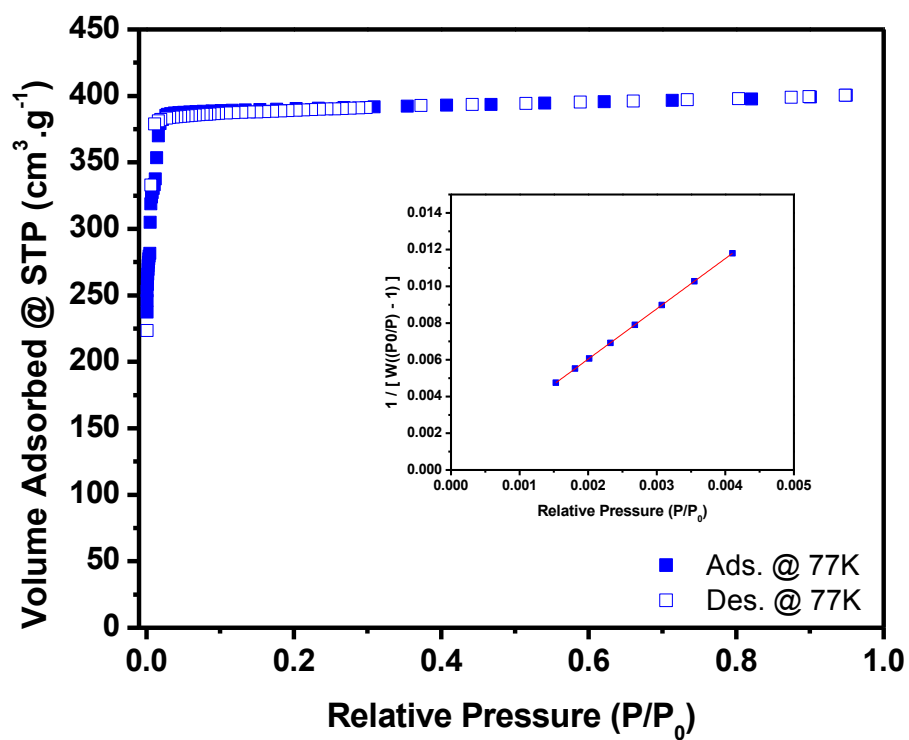
C: 3850.556

Qm: 365.4 cm³/g STP

Correlation Coefficient: 0.999997

Molecular cross sectional area: 0.1620 nm²

Figure S4. N₂ adsorption isotherm at 77 K. Inset: BET linear fit for ZIF-8 (size = 1.3 ± 0.2 μm) crystals.



BET surface area: 1271.611 m²/g STP

Slope: 2.738 g/cm³ STP

Y intercept: 0.0005607 g/cm³ STP

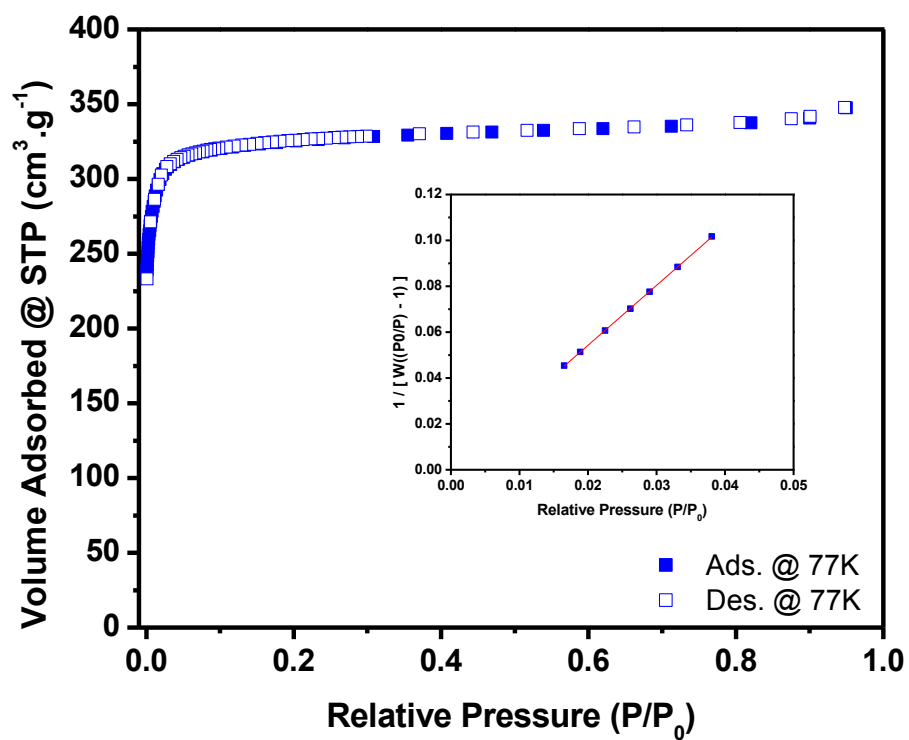
C: 4884.654

Q_m: 400.4 cm³/g STP

Correlation Coefficient: 0.999999

Molecular cross sectional area: 0.1620 nm²

Figure S5. N₂ adsorption isotherm at 77 K. Inset: BET linear fit for UiO-66 (size = 190 ± 22 nm) crystals.



BET surface area: 1332.052 m^2/g STP

Slope: 2.612 g/cm^3 STP

Y intercept: 0.002019 g/cm^3 STP

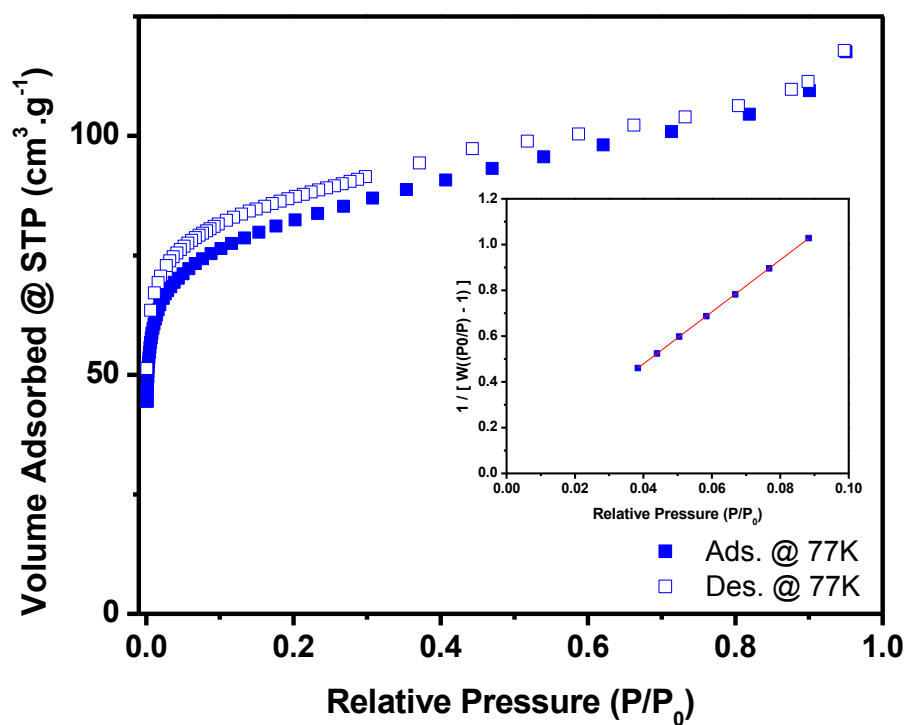
C: 1295.052

Qm: 347.39 cm^3/g STP

Correlation Coefficient: 0.999966

Molecular cross sectional area: 0.1620 nm^2

Figure S6. N₂ adsorption isotherm at 77 K. Insert: BET linear fit for UiO-66-SH (size = 208 ± 54 nm) crystals.



BET surface area: 305.877 m²/g STP

Slope: 11.361 g/cm³ STP

Y intercept: 0.02412 g/cm³ STP

C: 472.127

Qm: 117.61 cm³/g STP

Correlation Coefficient: 0.999993

Molecular cross sectional area: 0.1620 nm²

Figure S7. Photographs and representative FESEM images of the colloidal MOFs immobilized onto glass Ti/Au-thiol substrates ($\approx 2 \text{ cm} \times 2 \text{ cm}$). (a) ZIF-8 (size = $1.3 \pm 0.2 \mu\text{m}$), (b) ZIF-8 (size = $201 \pm 9 \text{ nm}$), (c) ZIF-8 (size = $101 \pm 10 \text{ nm}$), (d) UiO-66 (size = $190 \pm 22 \text{ nm}$), and (e) UiO-66-SH (size = $208 \pm 54 \text{ nm}$). Scale bars: $20 \mu\text{m}$ (left image) and $3 \mu\text{m}$ (right image).

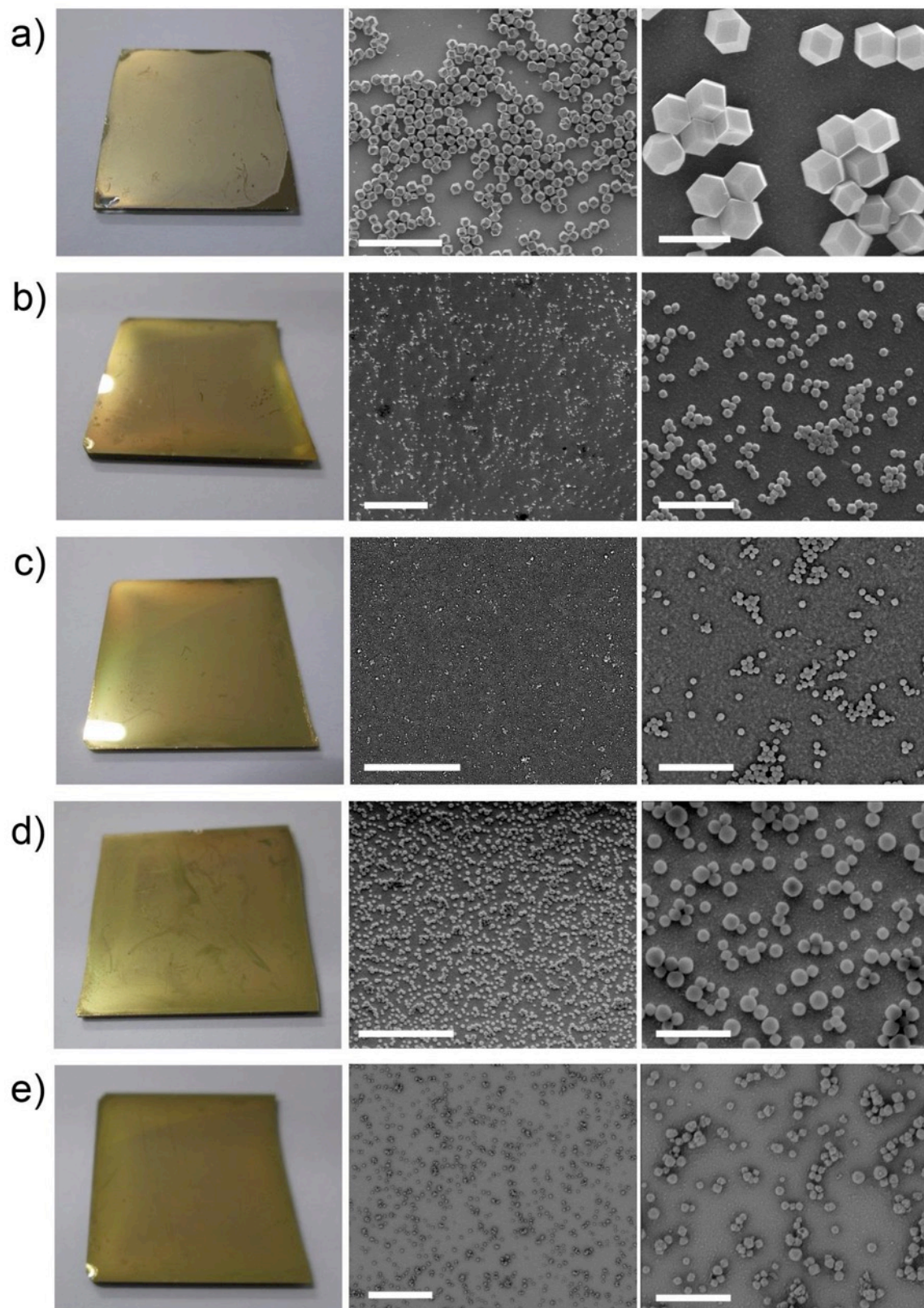


Figure S8. Representative FESEM images of (a) ZIF-8 (size = $1.3 \pm 0.2 \mu\text{m}$) crystals, (b) Janus Au@ZIF-8 particles (Au film thickness = 50 nm), and (c) Janus Au@ZIF-8 particles of different Au film thicknesses (5 nm, 10 nm, 20 nm, 30 nm or 50 nm). (d) Plot showing the average ($n = 5$) of the atomic percentage (measured by EDX) between Zn and Au in the Janus Au@ZIF-8 particles of different Au film thicknesses. Scale bars: $3 \mu\text{m}$ (a), $2 \mu\text{m}$ (b), and 500 nm (c).

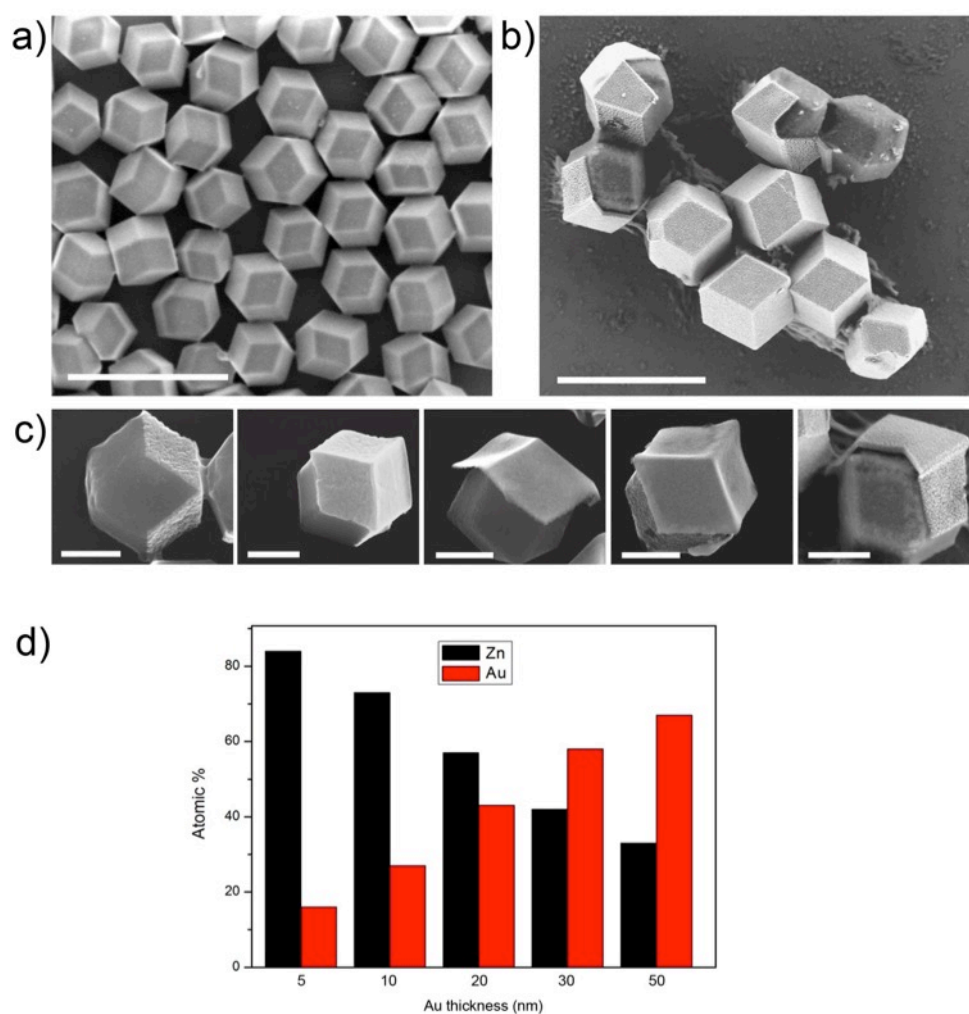


Figure S9. Representative FESEM images of (a) ZIF-8 (size = 201 ± 9 nm) crystals, (b) Janus Au@ZIF-8 particles (Au film thickness = 50 nm), and (c) Janus Au@ZIF-8 particles of different Au film thicknesses (5 nm, 10 nm, 20 nm, 30 nm or 50 nm). (d) Plot showing the average ($n = 5$) of the atomic percentage (measured by EDX) between Zn and Au in the Janus Au@ZIF-8 particles of different Au film thicknesses. Scale bars: 500 nm (a), 300 nm (b), and 100 nm (c).

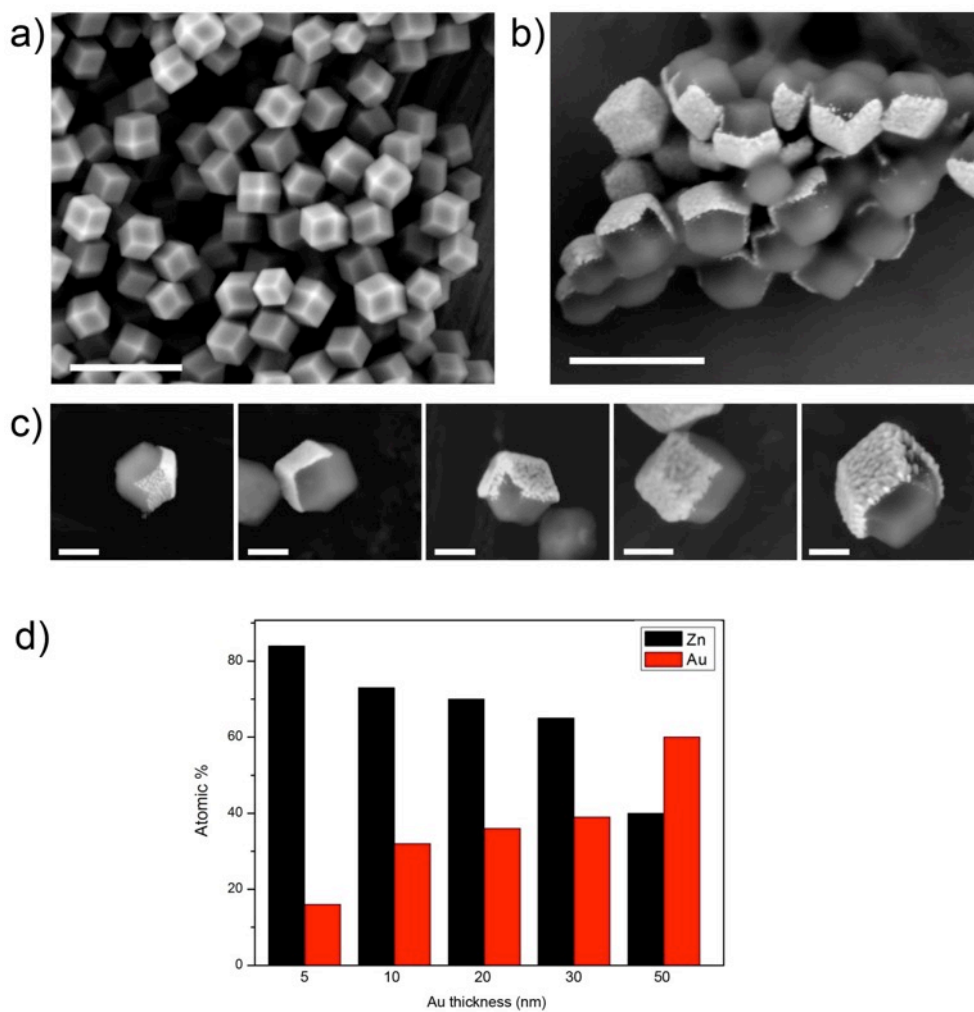


Figure S10. Representative FESEM images of (a) ZIF-8 (size = 101 ± 10 nm) crystals, (b) Janus Au@ZIF-8 particles (Au film thickness = 50 nm), and (c) Janus Au@ZIF-8 particles of different Au film thicknesses (5 nm, 10 nm, 20 nm, 30 nm or 50 nm). (d) Plot showing the average ($n = 5$) of the atomic percentage (measured by EDX) between Zn and Au in the Janus Au@ZIF-8 particles of different Au film thicknesses. Scale bars: 500 nm (a), 400 nm (b), and 100 nm (c).

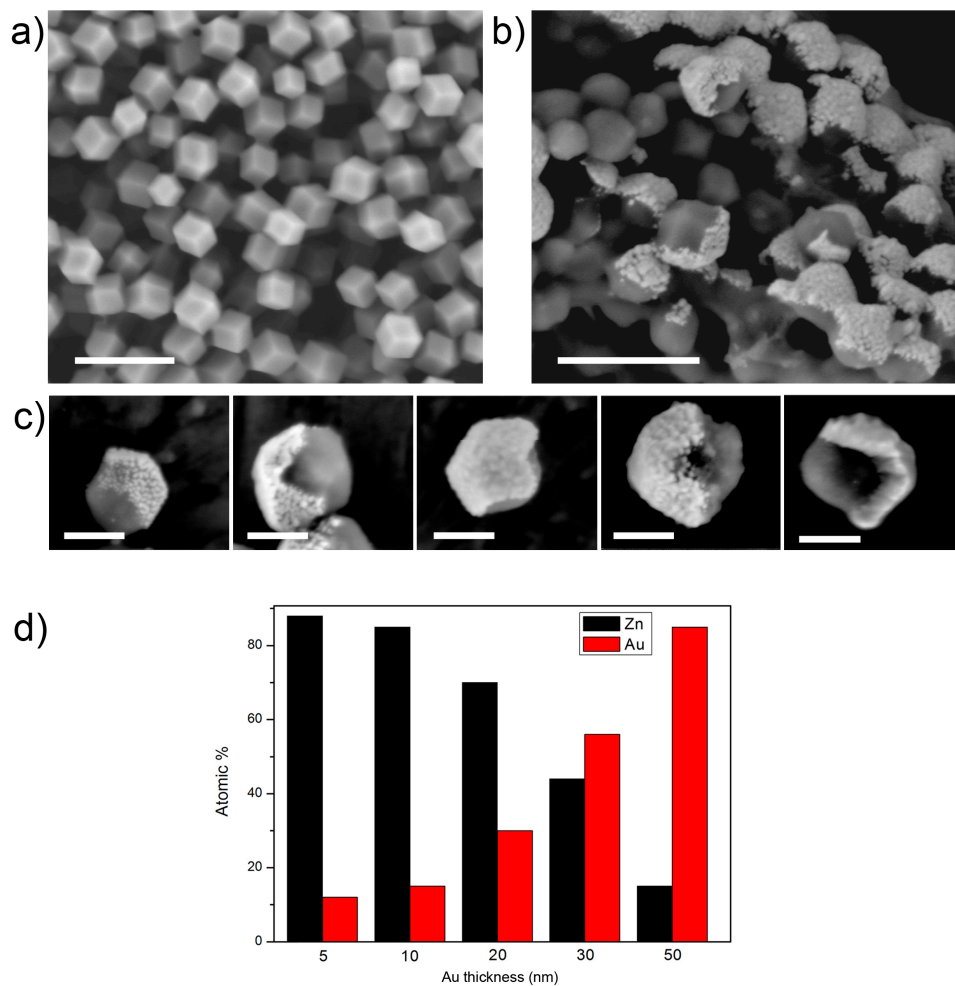


Figure S11. Representative FESEM images of (a) UiO-66 crystals, (b) Janus Au@ UiO-66 particles (Au film thickness = 50 nm), and (c) Janus Au@UiO-66 particles of different Au film thicknesses (5 nm, 10 nm, 20 nm, 30 nm or 50 nm). (d) Plot showing the average (n = 5) of the atomic percentage (measured by EDX) between Zn and Au in the Janus Au@UiO-66 particles of different Au film thicknesses. Scale bars: 500 nm (a,b), and 100 nm (c).

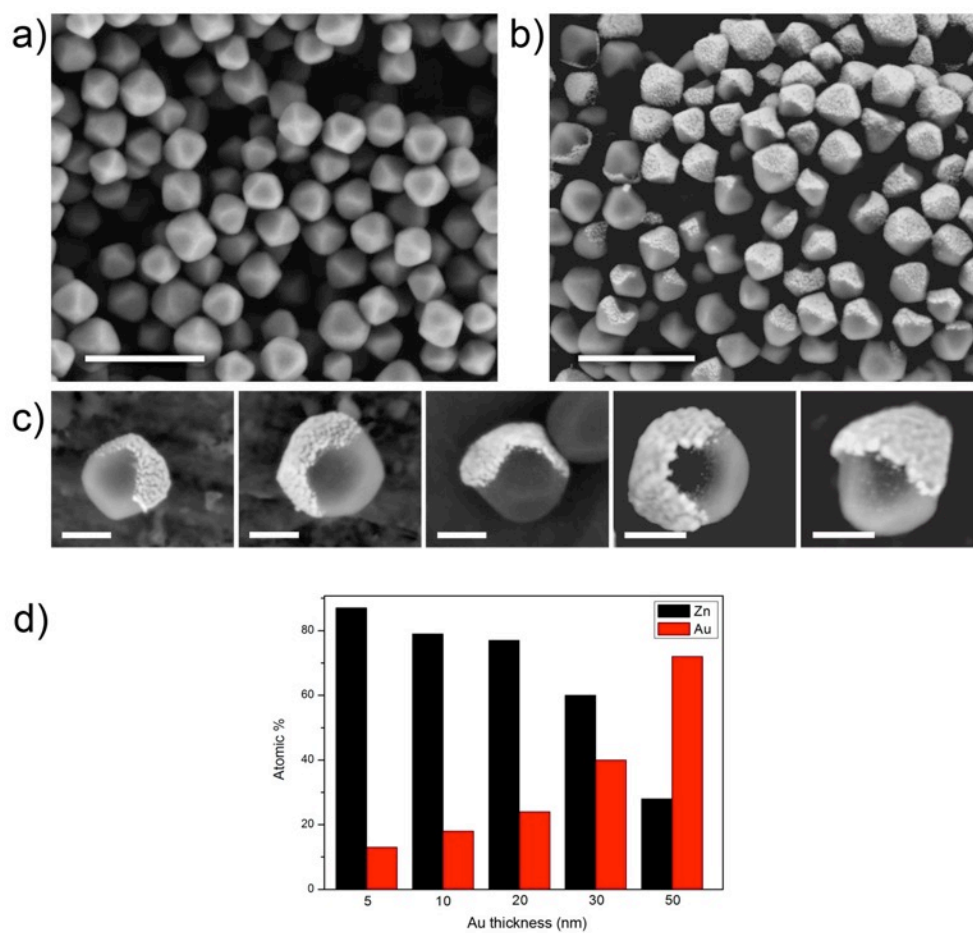


Figure S12. EDX mapping of (a) single Au@ZIF-8 (size = $1.3 \pm 0.2 \mu\text{m}$; Au film thickness = 50 nm) and (b) Au@UiO-66 (size = $190 \pm 22 \text{ nm}$; Au film thickness = 50 nm) particles showing the Zn or Zr (green) distribution and the Au (red) distribution.

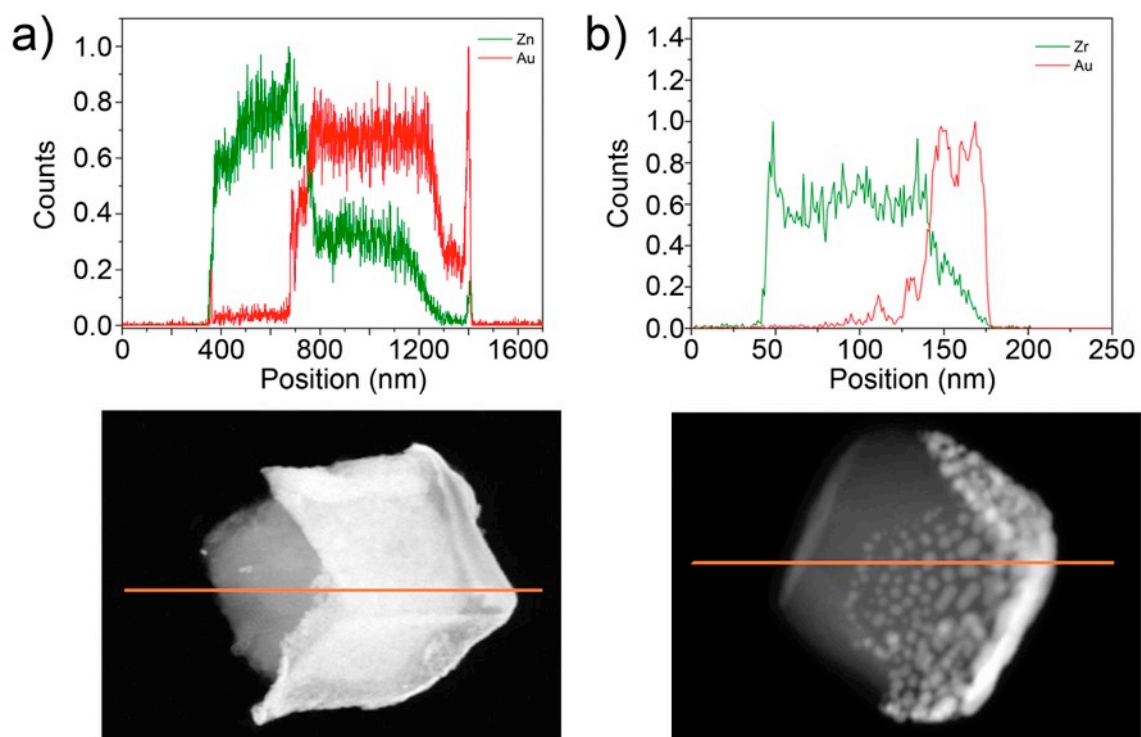


Figure S13. XRPD diffractograms of the Janus Au@ZIF-8 (size = 101 ± 10 nm) particles fabricated with different Au film thicknesses (5 nm, 10 nm, 20 nm, 30 nm or 50 nm), as compared to the simulated powder pattern for ZIF-8 and Au.

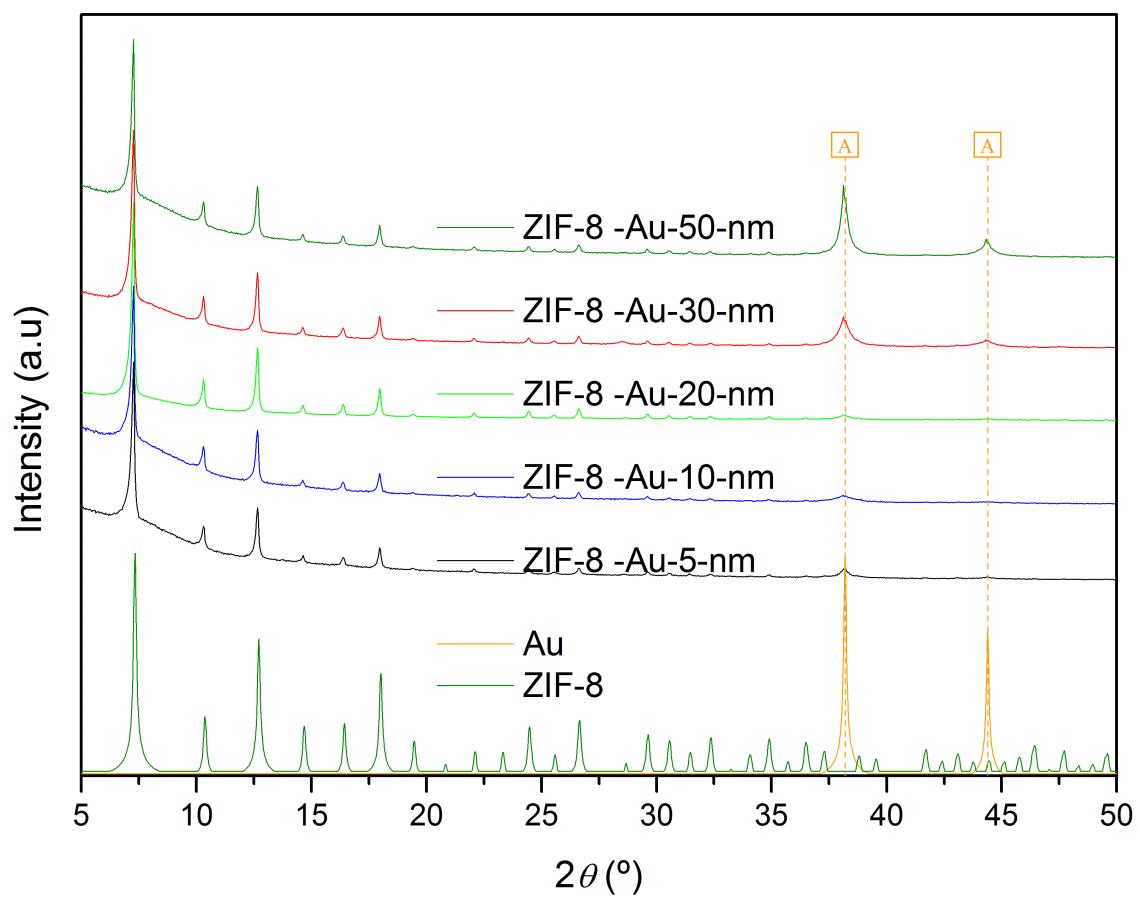


Figure S14. XRPD diffractograms of the Janus Au@ZIF-8 (size = 201 ± 9 nm) particles fabricated with different Au film thicknesses (5 nm, 10 nm, 20 nm, 30 nm or 50 nm), as compared to the simulated powder pattern for ZIF-8 and Au.

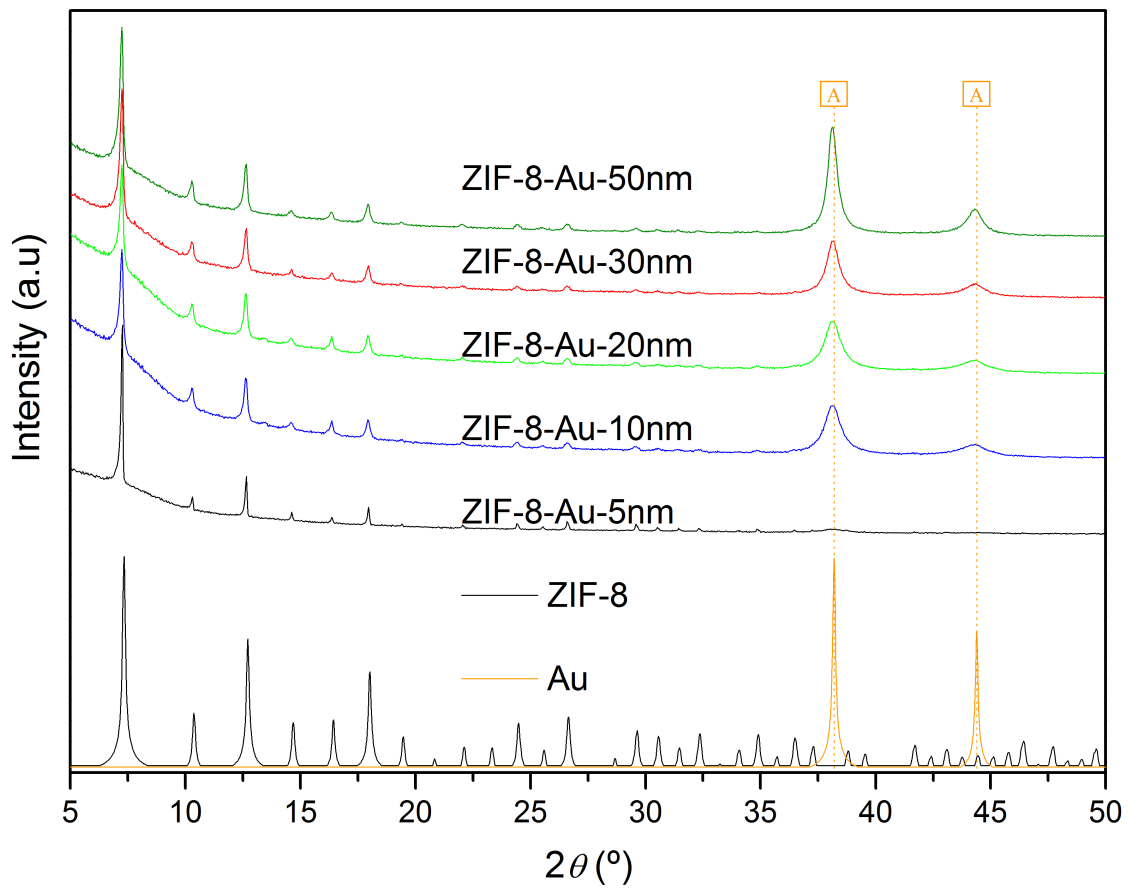


Figure S15. XRPD diffractograms of the Janus Au@ZIF-8 (size = $1.3 \pm 0.2 \mu\text{m}$) particles fabricated with different Au film thicknesses (5 nm, 10 nm, 20 nm, 30 nm or 50 nm), as compared to the simulated powder pattern for ZIF-8 and Au.

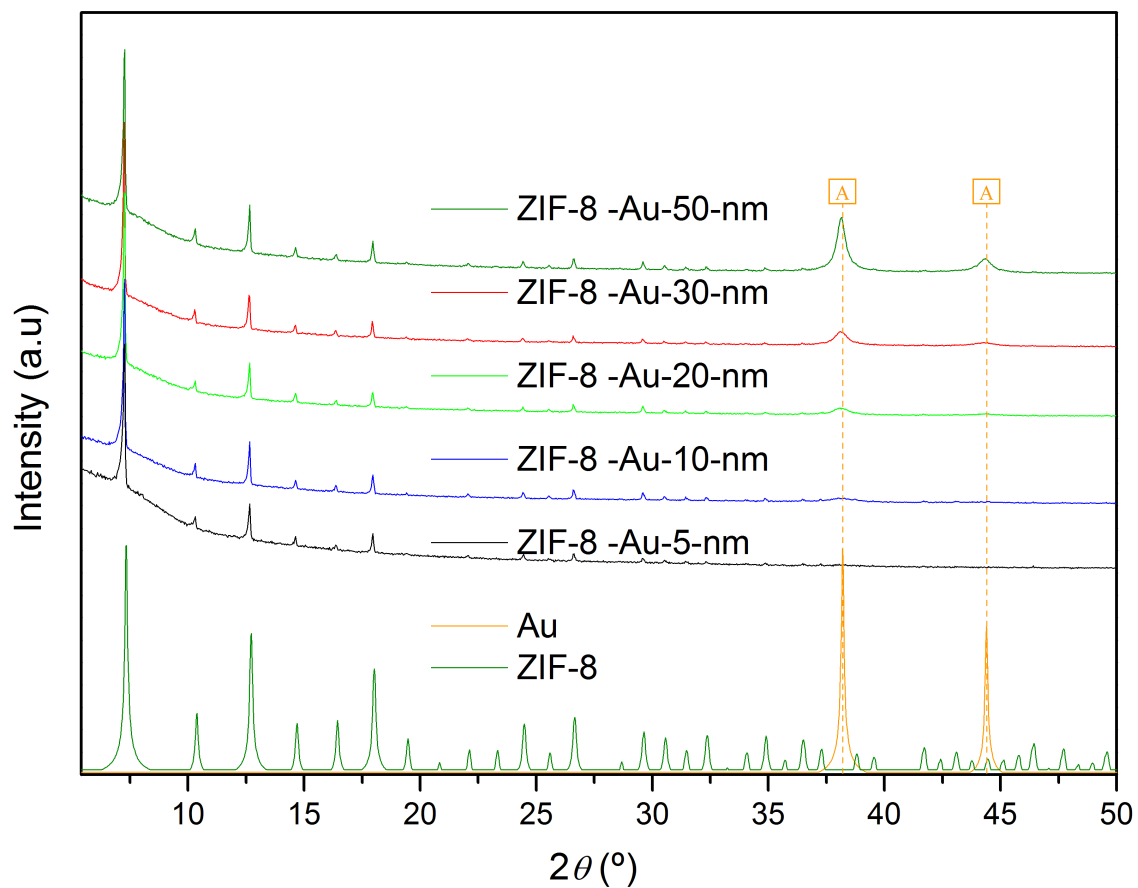


Figure S16. XRPD diffractograms of the Janus Au@UiO-66 (size = 190 ± 22 nm) particles fabricated with different Au film thicknesses (5 nm, 10 nm, 20 nm, 30 nm or 50 nm), as compared to the simulated powder pattern for UiO-66 and Au.

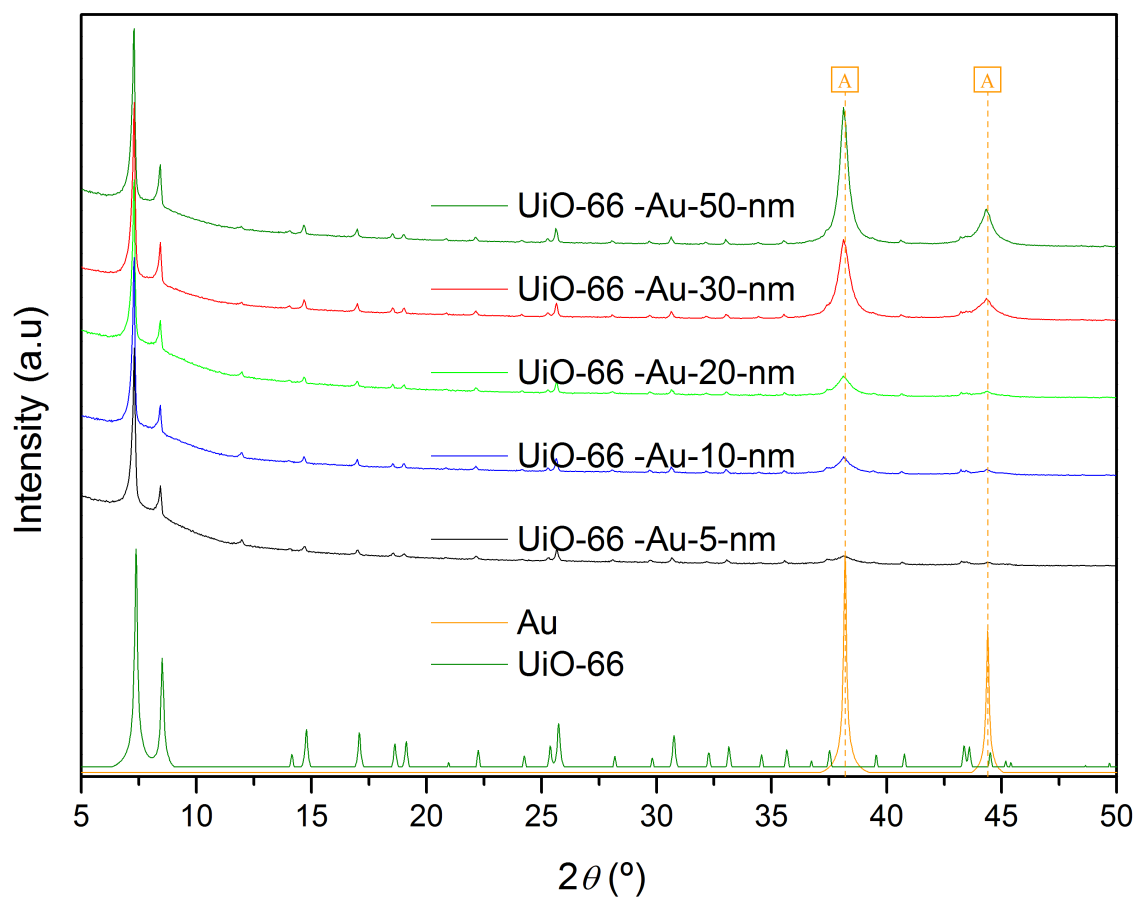
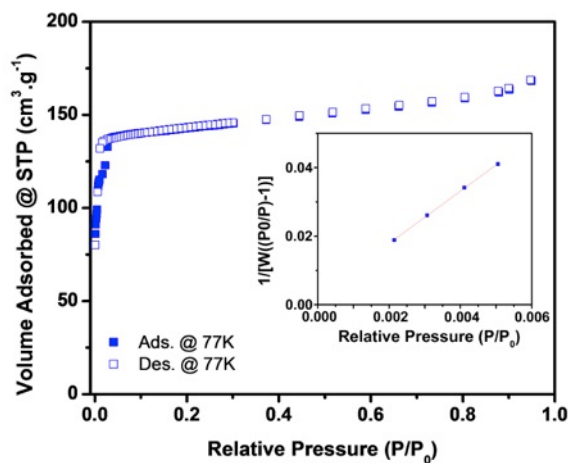


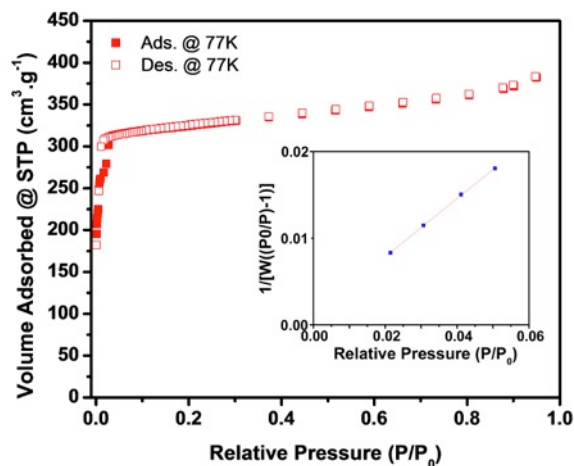
Figure S17. N₂ adsorption isotherms at 77 K and BET linear fit for Janus Au@ZIF-8 (size = 201 ± 9 nm; Au film thickness = 50 nm) particles expressed as expressed in m² per grams (a) Au@ZIF-8 and (b) ZIF-8 once we calculated the amount of Au present in the samples (56 % w/w) by selectively dissolving the ZIF-8 component using an aqueous HCl solution (pH < 1).

a)



BET surface area: 456.392 m²/g STP
 Slope: 7.628 g/cm³ STP
 Y intercept: 0.002639 g/cm³ STP
 C: 2891.689
 Qm: 168.21 cm³/g STP
 Correlation Coefficient: 0.999858
 Molecular cross sectional area: 0.1620 nm²

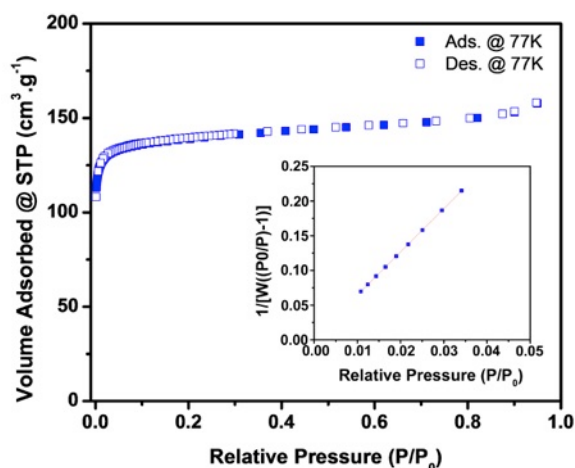
b)



BET surface area: 1037.254 m²/g STP
 Slope: 3.356 g/cm³ STP
 Y intercept: 0.001161 g/cm³ STP
 C: 2891.689
 Qm: 382.38 cm³/g STP
 Correlation Coefficient: 0.999858
 Molecular cross sectional area: 0.1620 nm²

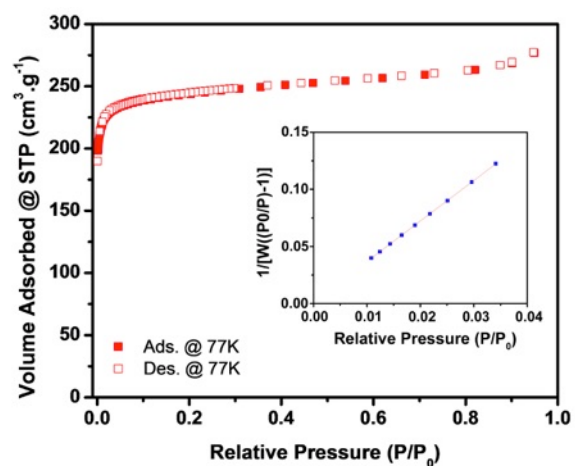
Figure S18. N₂ adsorption isotherms at 77 K and BET linear fit for Janus Au@UiO-66 (Au film thickness = 5 nm) particles expressed in m² per grams (a) Au@UiO-66 and (b) UiO-66, once the amount of Au present in the sample (43% w/w) had been calculated upon selectively dissolving the UiO-66 component using an aqueous H₂SO₄ solution (pH < 1).

a)



BET surface area: **559.750** m²/g STP
 Slope: 6.219 g/cm³ STP
 Y intercept: 0.002447 g/cm³ STP
 C: 2542.985
 Qm: 157.73 cm³/g STP
 Correlation Coefficient: 0.999992
 Molecular cross sectional area: 0.1620 nm²

b)



BET surface area: **982.018** m²/g STP
 Slope: 3.545 g/cm³ STP
 Y intercept: 0.001395 g/cm³ STP
 C: 2542.985
 Qm: 276.72 cm³/g STP
 Correlation Coefficient: 0.999992
 Molecular cross sectional area: 0.1620 nm²

Figure S19. Representative confocal image (with two channels: ZIF-8, blue (λ excitation = 405 nm, λ emission = 420 nm to 490 nm); FITC-PEG-SH, green (λ excitation = 488 nm, λ emission = 500 nm to 550 nm) and corresponding 3D image showing the asymmetric functionalization of a single Janus FITC-PEG-S-Au@ZIF-8 (size = $1.3 \mu\text{m} \pm 0.2 \mu\text{m}$) particle. Image was treated in Imaris 3D software, version 6.1.0.

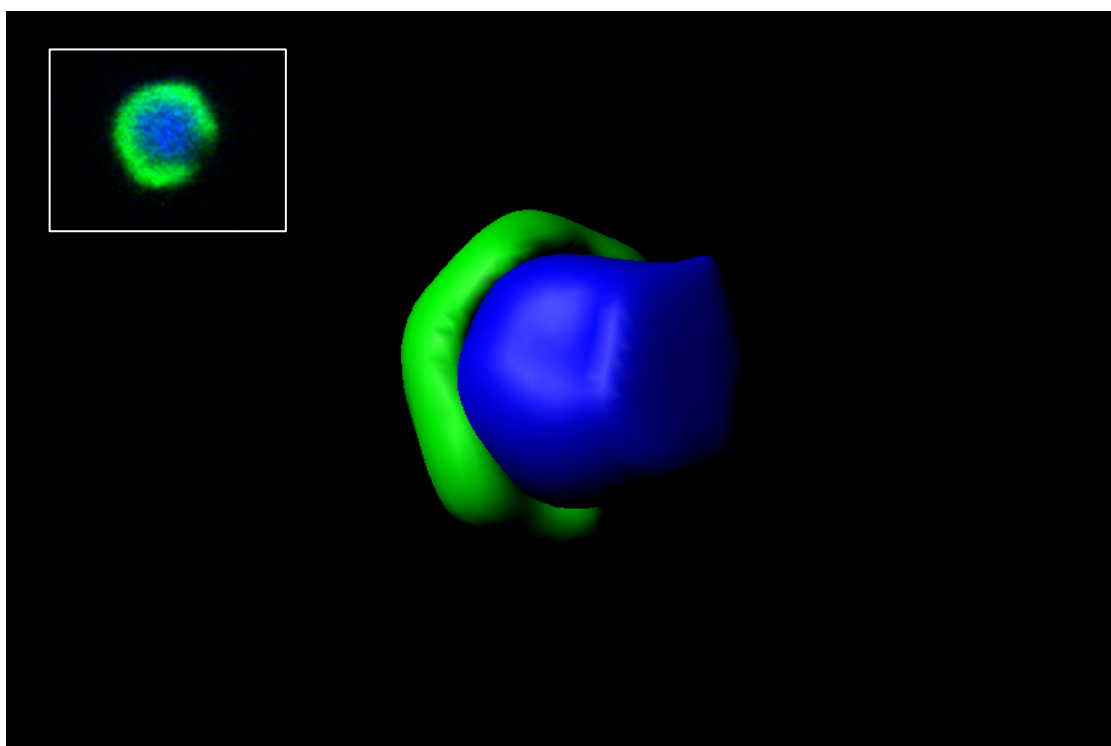


Figure S20. EDX mapping of a single Co@ZIF-8 (size = 201 ± 9 nm; Co film thickness = 20 nm) particle showing the Zn (green) and Co (red) distribution.

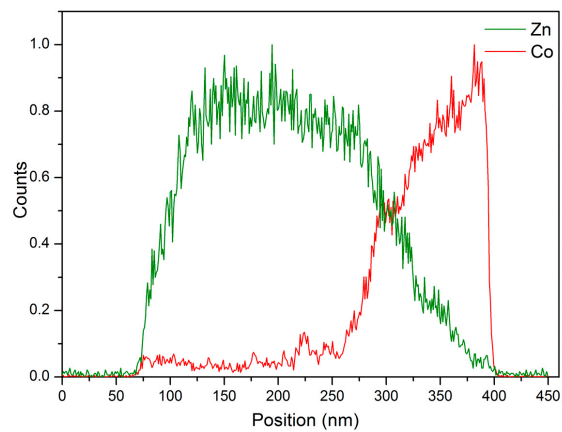
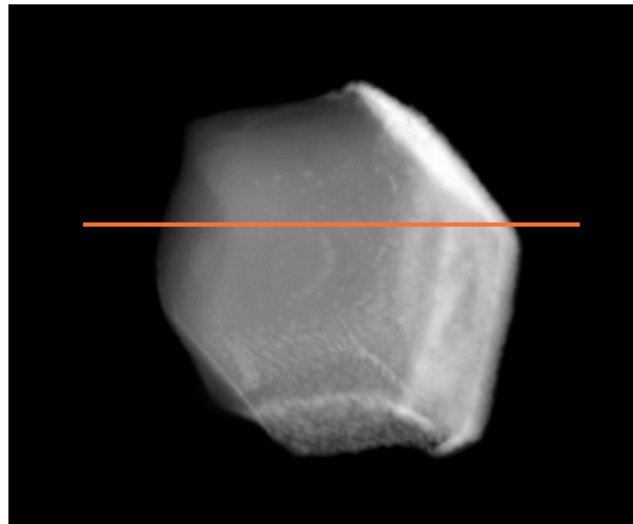


Figure S21. EDX mapping of a single Co@UiO-66 (Co film thickness = 20 nm) particle showing the Zr (green) and Co (red) distribution.

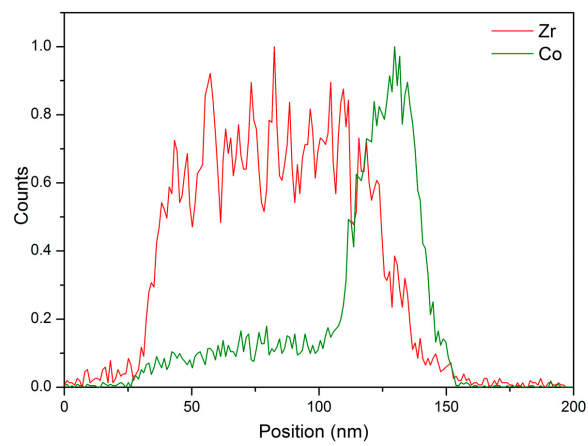
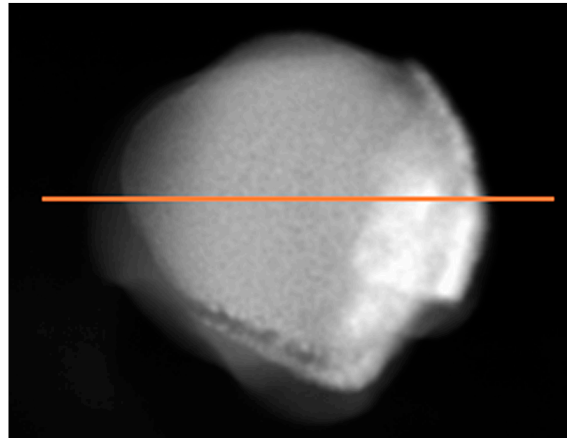


Figure S22. XRPD diffractograms of the Janus Co@ZIF-8 (size = 201 ± 9 nm; Co film thickness = 20 nm) particles, as compared to the simulated powder pattern for ZIF-8 and Co.

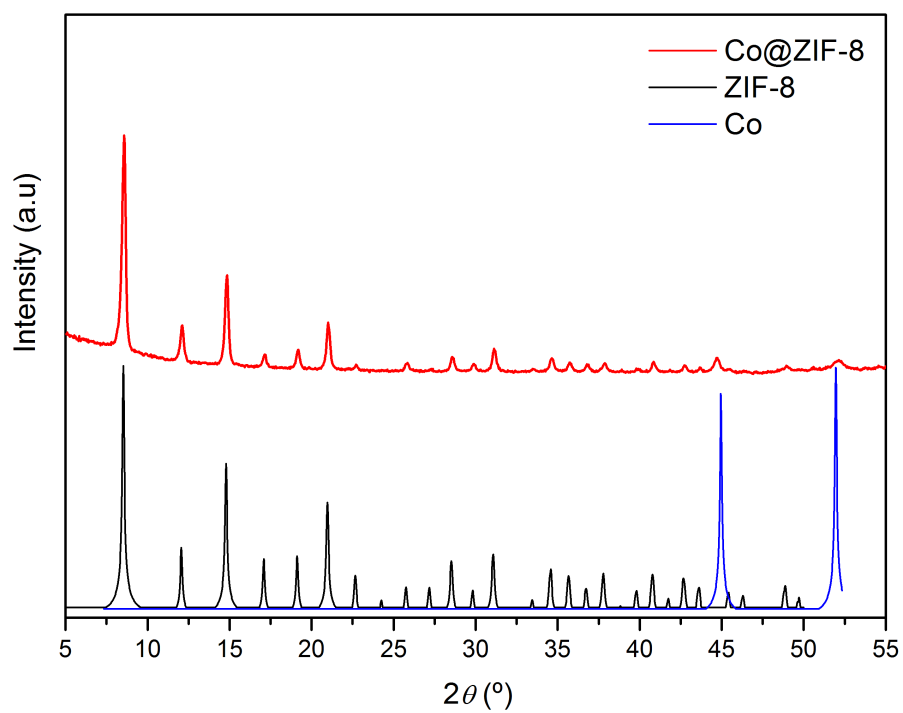


Figure S23. XRPD diffractograms of the Janus Co@UiO-66 (Co film thickness = 20 nm) particles, as compared to the simulated powder pattern for UiO-66 and Co.

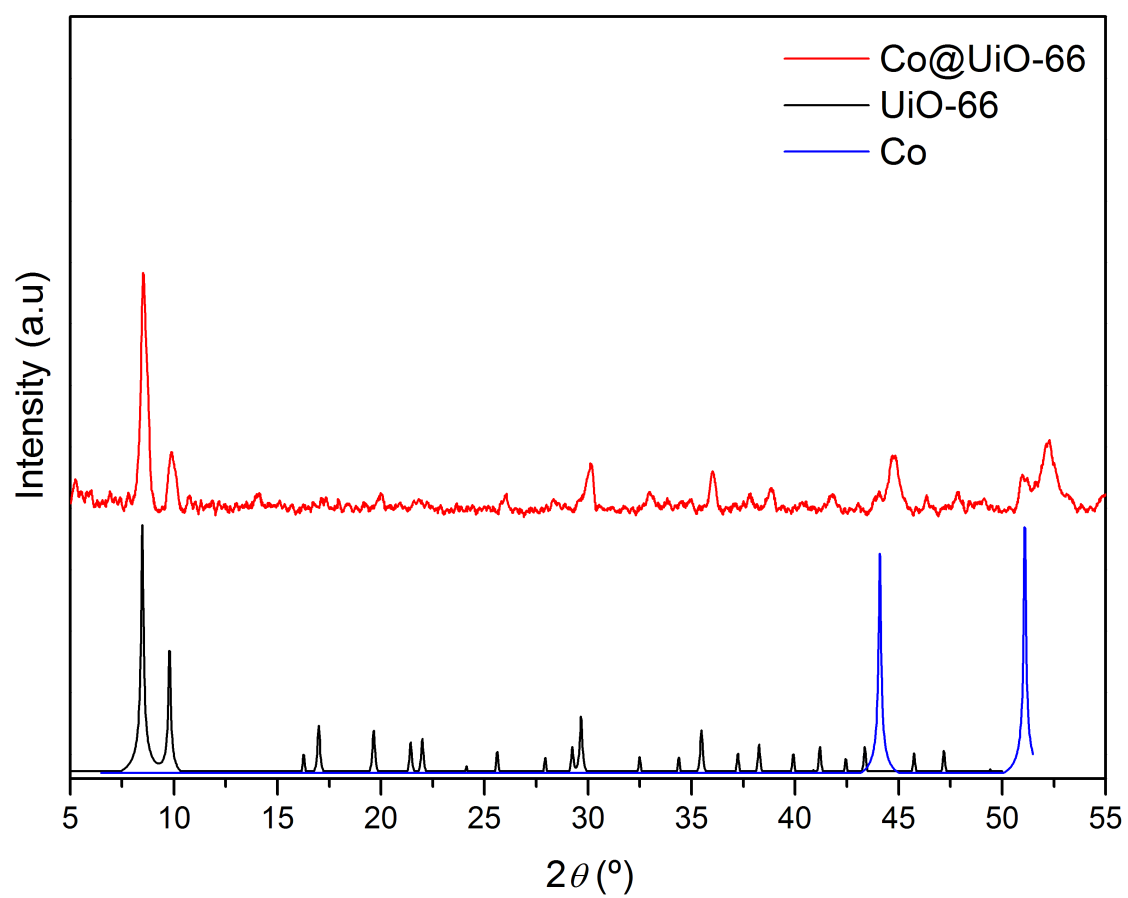


Figure S24. XRPD diffractograms of the Janus Co@UiO-66-SH (Co film thickness = 20 nm) particles, as compared to the simulated powder pattern for UiO-66 and Co.

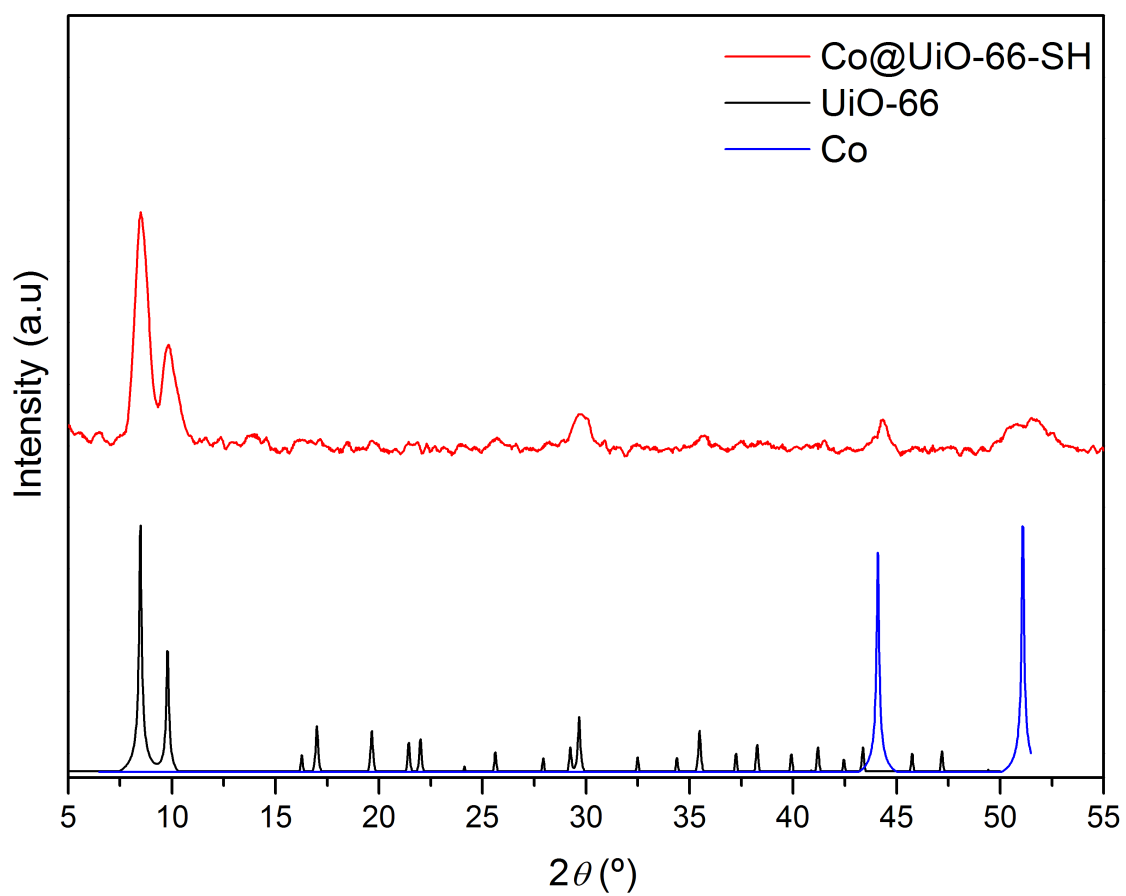


Figure S25. Magnetic hysteresis loop measured at 300 K. (a) Janus Co@ZIF-8 (size = 201 ± 9 nm), b) Co@UiO-66, c) Co@UiO-66-SH, and d) Au@Co@UiO-66.

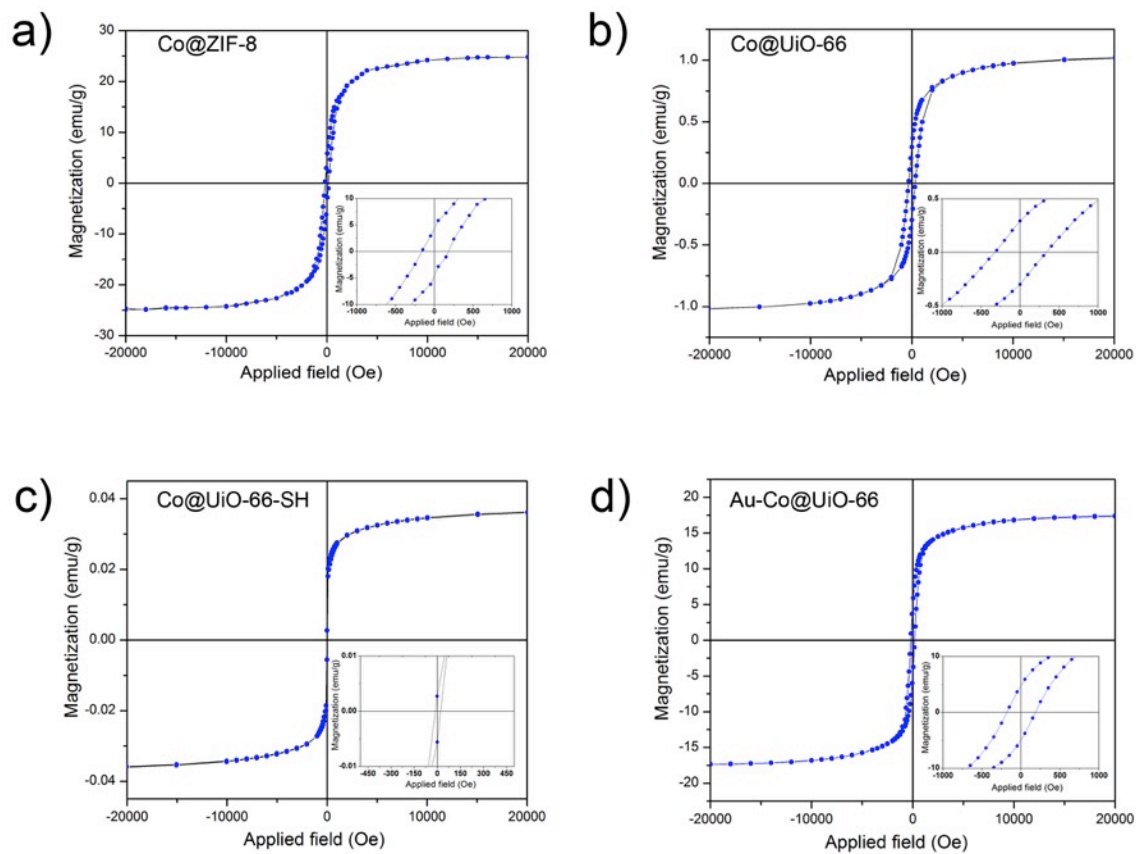


Figure S26. EDX mapping of a single Pt@ZIF-8 (size = $1.3 \mu\text{m} \pm 0.2 \mu\text{m}$; Pt film thickness = 20 nm) particle showing the Zn (green) and Pt (red) distribution.

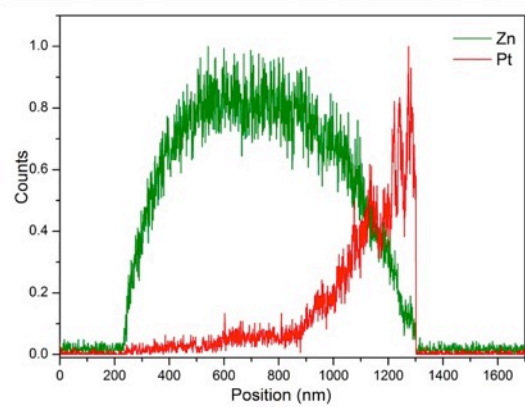
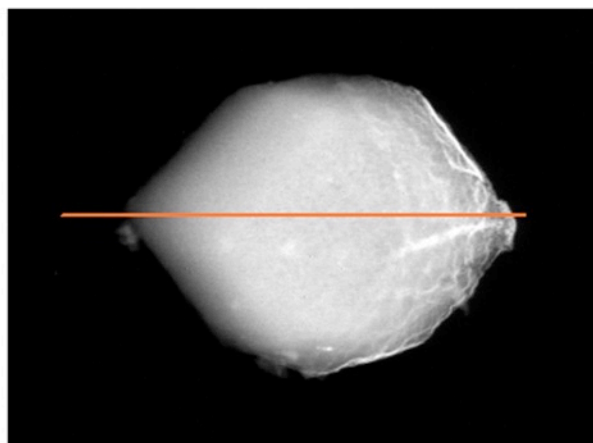


Figure S27. XRPD diffractograms of Janus Pt@ZIF-8 (size = $1.3 \mu\text{m} \pm 0.2 \mu\text{m}$; Pt film thickness = 20 nm) particles, as compared to the simulated powder pattern for ZIF-8 and Pt.

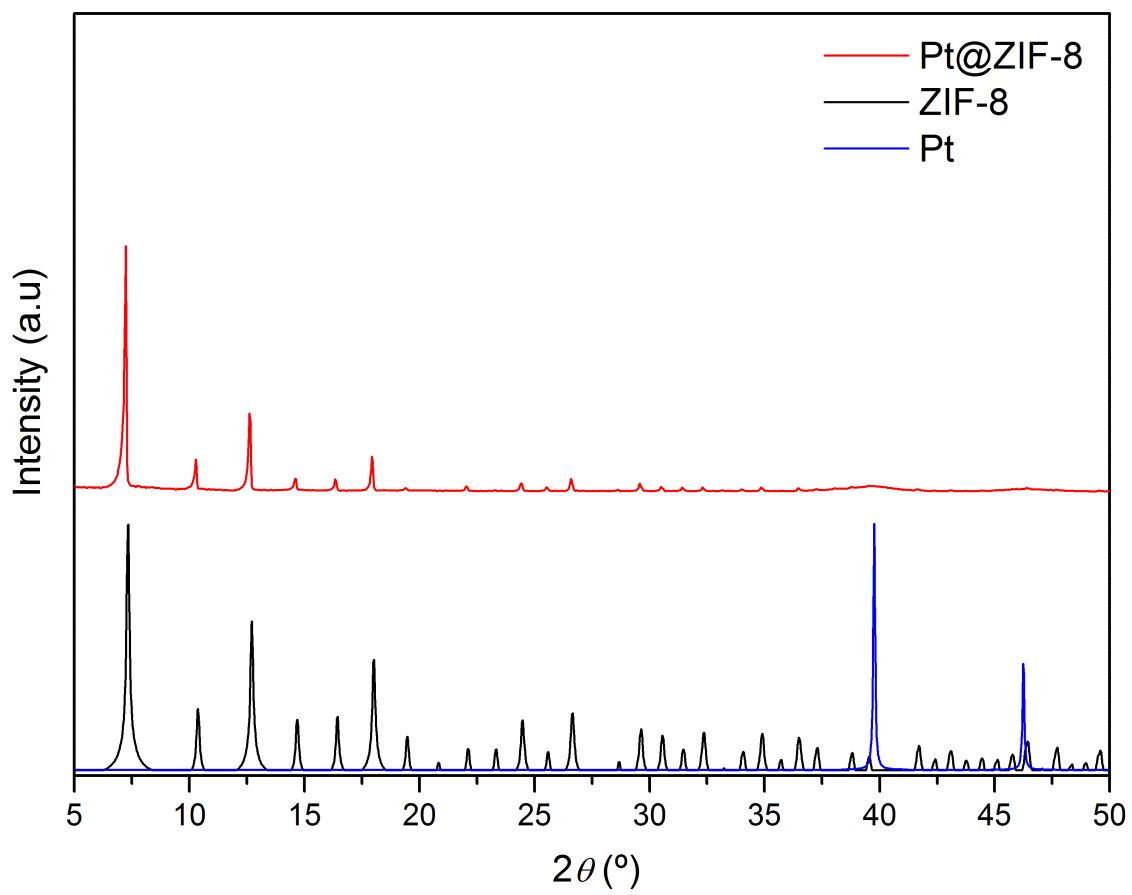


Figure S28. XRPD diffractograms of Janus bimetallic Au@Co@UiO-66 (Co film thickness = 20 nm; Au film thickness = 5 nm) particles, as compared to the simulated powder pattern for UiO-66, Au and Co.

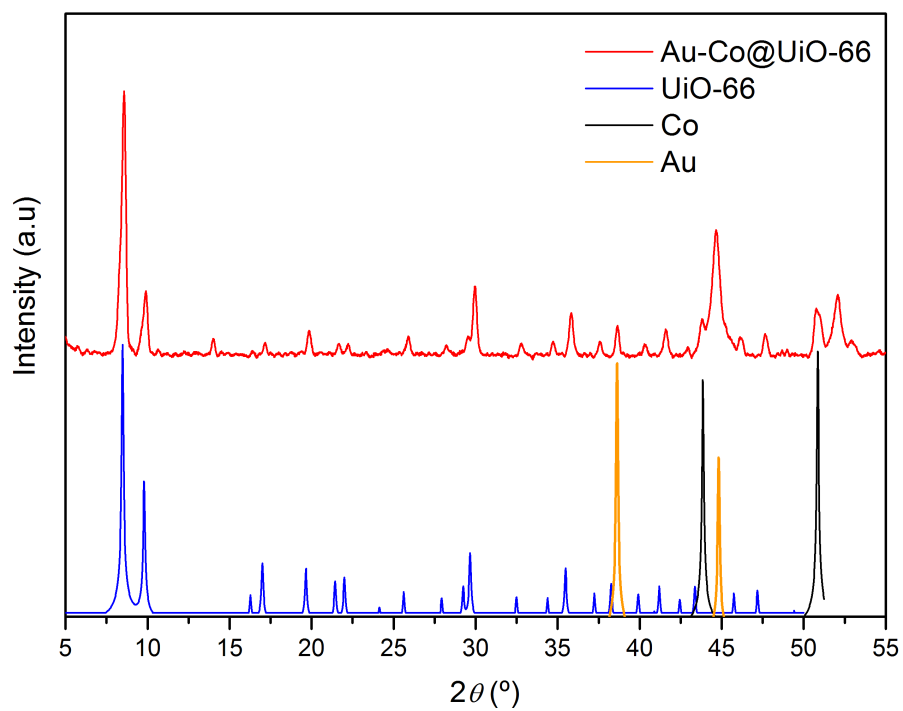


Figure S29. Bimetallic Janus Au@Co@UiO-66 (Co film thickness = 20 nm; Au film thickness = 5 nm) particles. (a) Confocal image confirming functionalization of the particles with the green fluorophore FITC-PEG-SH. (b) Photograph confirming the magnetic attraction of these particles to a magnet.

